

Comparison of silicon potentials for cluster bombardment simulations

J. Samela ^{a,*}, K. Nordlund ^a, J. Keinonen ^a, V.N. Popok ^b

^a Accelerator Laboratory, University of Helsinki, P.O. Box 43, 00014 University of Helsinki, Finland

^b Department of Physics, Gothenburg University, 41296 Gothenburg, Sweden

Available online 10 January 2007

Abstract

We have compared three common silicon potentials for molecular dynamics simulations of cluster bombardment of silicon structures. The potentials tested are Stillinger–Weber, Tersoff III and EDIP. We have also tested one variation of Stillinger–Weber and a variation of Tersoff III potential to see how small modifications of parameter values affect collision cascade and crater geometries. Single ion sputtering yields are compared to experimental values. In simulations, Si(111) surfaces are bombarded with 1–60 keV Ar₁₂ clusters. The potentials give almost similar overall description of collision cascades at different energies. However, measurable quantities like sputtering yields and crater sizes vary considerably between potentials and even between different parametrisations of the same potential.

© 2006 Elsevier B.V. All rights reserved.

PACS: 34.20.Cf; 34.50.Dy; 79.20.Ap; 79.20.Rf; 61.46.Bc; 61.80.Jh

Keywords: Interatomic potential; Sputtering; Collision cascade; Molecular dynamics; Ion irradiation; Atomic cluster; Cratering

1. Introduction

The collision of an energetic noble gas cluster with a silicon surface is one of the most complex dynamical phenomena that can be studied using molecular dynamics simulations. The reliability of simulations depends considerably on the applicability of interatomic potential to dynamics of collision cascades.

Interatomic potentials for silicon are developed, tested, compared and applied extensively because of the great industrial importance of silicon. In addition, pure crystalline and amorphous silicon structures are ideal platforms for basic research of covalently bonded materials. Increasing computing power has made it possible to simulate not only static structures, but more and more complex and dynamic phenomena like collision cascades caused by energetic cluster bombardment. However, the interatomic potentials are originally constructed for simulation of solid phases of silicon. Therefore, it is not evident, whether one

can make precise conclusions on the dynamics of cluster collision cascades based on simulations with one potential.

The potentials are traditionally tested against experimental properties like bulk moduli and phonon frequencies. However, there is not very much precise experimental data about collision cascades and the traces they leave on surfaces. Sputtering yields for ion bombardment are available, and comparing simulated yields against experimental yields provides one way to verify potentials for collision cascade simulations. Scanning probe and transmission electron microscopies provides a new opportunity to measure real crater structures on an atomic level [1–3].

It is agreed that no single empirical potential can be expected to fully reproduce the crystalline, amorphous, and liquid behavior of silicon [4,5]. A good potential for cluster bombardment simulations should fulfill at least the following three requirements. Firstly, the potential should describe the all three phases reasonably well, because the phases co-exist in collision cascades. For example, if the potential describes very well the crystalline and amorphous phases but is unphysical in liquid phase, it is not valid for the collision cascade simulations. Secondly, a good potential should produce phase transitions at

* Corresponding author. Tel.: +358505567176; fax: +35898884952.

E-mail address: juha.samela@helsinki.fi (J. Samela).

temperatures close to the experimental values. If the melting temperature is too high, collision cascade will develop slower and it will be smaller than in the case of the right melting temperature. The third requirement is that a good potential should realistically model binding of atoms on surfaces. If the binding is too weak, the crater rims will rather sputter than form surface structures.

The potentials are based on partially different models of covalent bonding. Comparison of potentials provides an opportunity to reason, which features and parameters of these models affect cascade and crater geometry, as well as sputtering. Many comparisons of silicon potentials are published. The comparisons indicate that there are remarkable differences in how the potentials describe different phases of silicon. Some comparisons relevant to collision cascades are referenced later in this paper.

2. Potentials

Five potentials were tested. Three of them are original versions and two are modifications. All potentials have two-body attractive parts and three-body parts which model the spatial orientation of covalent bonds between silicon atoms.

The Stillinger–Weber potential (abbreviated SW in this paper) has two-body part V_2 and three-body contribution V_3 which weakens the attraction between silicon atoms in directions that are not ideal bonding angles [6,7].

$$V = V_2 + V_3 = \epsilon A \left[\sum_{(ij)} v_{ij}^{(2)}(r_{ij}) + \frac{\lambda}{A} \sum_{(jik)} v_{jik}^{(3)}(\bar{r}_{ij}, \bar{r}_{ik}) \right]. \quad (1)$$

SW describes crystalline, amorphous and liquid phases rather well [8–11]. An important fact regarding collision cascade simulations is that SW reproduces the melting temperature of the crystalline phase close to the experimental value [12,8,11].

The modified Stillinger–Weber potential (SWM) is intended to improve the description of the amorphous phase [5]. The modifications are obtained by a direct fit to the amorphous structure. The parameter λ in Eq. (1) has value 31.5 instead of the original value 21.0 and ϵ is changed from 2.16826 to 1.64833. This potential is included in the comparison because, in simulations, the collision cascades form an amorphous region inside the crystal and amorphous rims above its surface. However, SWM is not a good model for the liquid state of Si [4,5].

The Tersoff potential (TER) is a two-body Morse type potential with coefficients adjustable according to the number and position of neighbors of an atom pair. The potential has two parametrizations, one that gives good elastic properties and the other that gives good surface properties [13,14]. The potential used in this comparison is the former, which is often called Tersoff III. The choice was made because cluster impacts bring about pressure in the environment, and the pressure releases into elastic oscillations of the crystal lattice. The oscillations of lattice around col-

lision cascade presumably affects sputtering and crater shapes.

The parameters of the Tersoff potential are fitted to a large *ab initio* database of different structures of silicon, but not to any liquid phase data. The potential is found to overestimate greatly the melting point of silicon [15]. However, it describes various silicon crystal structures rather well [10].

The modified Tersoff potential (TERM) used in this comparison has a longer range for pair potential (3.5 Å) than the original potential (2.85 Å). Without this modification, Tersoff III has the shortest range among many silicon potentials [10]. The longer range may affect sputtering and surface structure formation, because the atoms about to leave the surface stay longer as a subject of attraction, for example.

SW and TER are found to give different bond angle distributions for liquid silicon. Bond angle distribution and dynamical properties of TER is closer to results of *ab initio* calculations [16]. Thijsse et al. have shown, that SW gives different energies per atom for various geometries possibly existing in collision cascades than density functional calculations [17]. SW and TER give a fair overall description of the structures and energetics of intrinsic defects and Si(100) surface, but do not model the Si(111) surface very well [10].

The environment-dependent interatomic potential (EDIP) has a fairly similar functional form for the two-body interaction as the SW potential, but it is modified according to the local coordination of the atoms [18]. It describes the crystalline phase, amorphous phase and point defects very well, among other good features. However, the melting point is about 20% below the experimental value, and the liquid phase has some unphysical features.

3. Simulation methods

In the cluster bombardment runs, a rectangular simulation lattice contained 1013760 silicon atoms arranged in the diamond structure. A smaller lattice consisting of 64000 atoms was used in single ion bombardments. One Si(111) surface was open and the clusters were targeted towards it perpendicularly. The initial position of a cluster within an area of one Si(111) unit cell and the cluster's initial rotational position are chosen randomly. Periodic boundary conditions were used at the sides of the simulation cell.

Berendsen temperature control was used to cool the sides and the bottom of the simulation cell to 300 K. The relatively large number of atoms, cooling regions and periodic boundary conditions together form a systems which prevents shock waves reflecting back to the collision cascade region and disturb its development. This topic and the cooling arrangement is discussed in [19].

The initial lattice was first simulated for 30 ps keeping the temperature at 300 K and pressure at zero and letting the volume of the lattice change. After that, one side was

opened, and the surface was relaxed in another 30 ps simulation. Simulation lattices for all potentials were prepared in this way separately.

In addition to the silicon potentials, a short range repulsive ZBL potential [20] was used to prevent high energy atoms moving too close to each other. Electronic stopping was applied as a non-local frictional force to all atoms having a kinetic energy larger than 10 eV [21,20]. 1–60 keV Ar₁₂ clusters were used in the simulations. The clusters were prepared using a Lennard-Jones potential.

The collision cascades were simulated for 30–50 ps depending on the cluster energy. After that, no structural changes that could affect the main results were observed in test runs with extended simulation time. In reality, some relaxation of crater rims and crystallization of amorphous regions might occur, but simulation of these long term effects are beyond the possibilities of molecular dynamics.

The experimental sputtering yields used in the comparison are measured with polycrystalline targets. Therefore, in the single ion collision simulations, the ion is targeted to the Si(111) surface in an angle which in average corresponds the approaching angles to the surfaces of a polycrystalline target. If the ion was targeted perpendicularly to the Si(111), the simulated sputtering yields would be considerably lower than the experimental yields. This is in line with the common practice of using a non-channeling direction to minimize channeling effects, to mimic bombardment of a polycrystalline target where the likelihood of entering a channel is small.

4. Results and discussion

Sputtering yields of single Ar ion bombardment simulations are shown in Fig. 1. Each point represents the average of 48 simulations. Experimental yield values originate from several sources and are combined in [22]. SW and TER give lower yields than EDIP, SWM and TERM and also too low yield compared to the experimental values. All potentials produce similar qualitative dependence between sputtering yield and ion energy up to about 20 keV. The dependence is also similar to the experimental dependence. Because of large errors in averages at energies higher than 20 keV, no conclusions can be made whether or not the yields follow the experimental curve at high energies.

Sputtering yields of Ar₁₂ cluster collisions onto Si(111) surface in Fig. 2 show clearly how changes of the parameters can change the results considerably. The stronger three-body interaction in SWM weakens bonding between atoms in certain directions and atoms are easily sputtered from the surface. Crater rims become also higher (Fig. 3). On the other hand, the increased range of TERM decreases sputtering yields compared to the original Tersoff potential. Even the energy dependence is different, and does not show the typical clear maximum. As Fig. 4 shows, TERM produces crater rims but no real craters. Therefore, we conclude that it binds, due to its longer range, the collision cascade atoms, which otherwise would evaporate out of

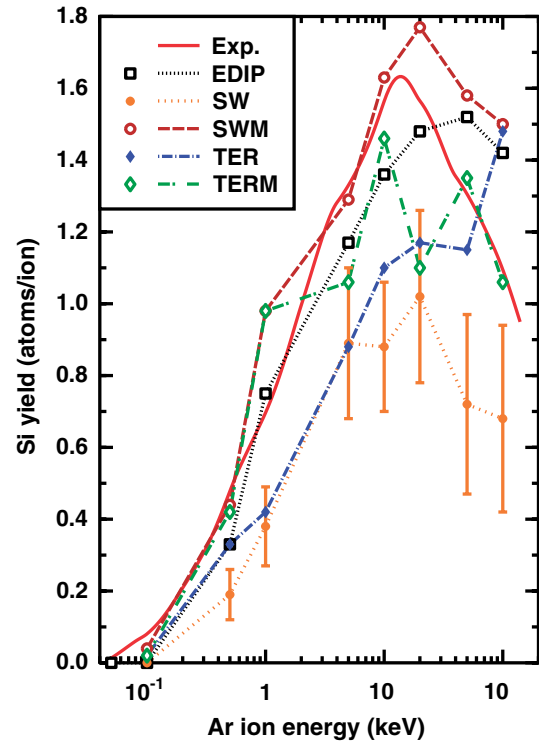


Fig. 1. Average Si sputtering yields after Ar ion impacts and comparison to experimental yields [22]. Each point represents an average of 48 simulations. For clarity, error bars are not shown for all simulated points.

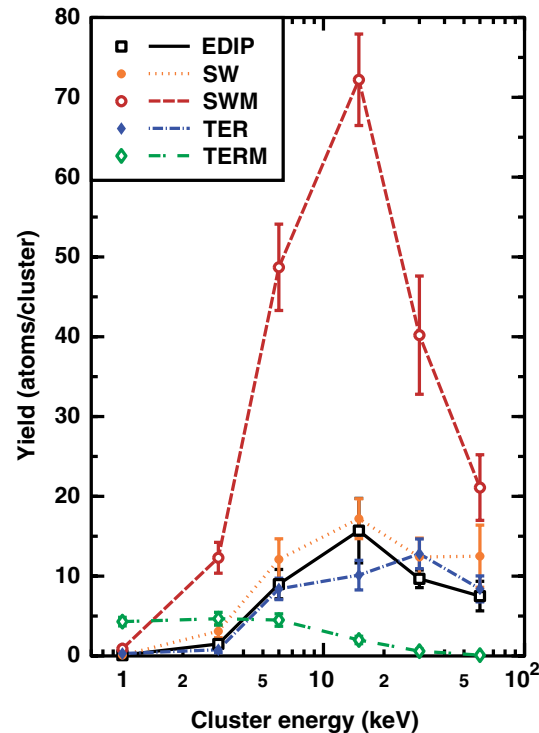


Fig. 2. Average Si sputtering yields in Ar₁₂ cluster collisions.

the center of collision cascade. This kind of sputtering due to thermal energy is visible in cluster impact simulations but it is not so significant sputtering mechanism in

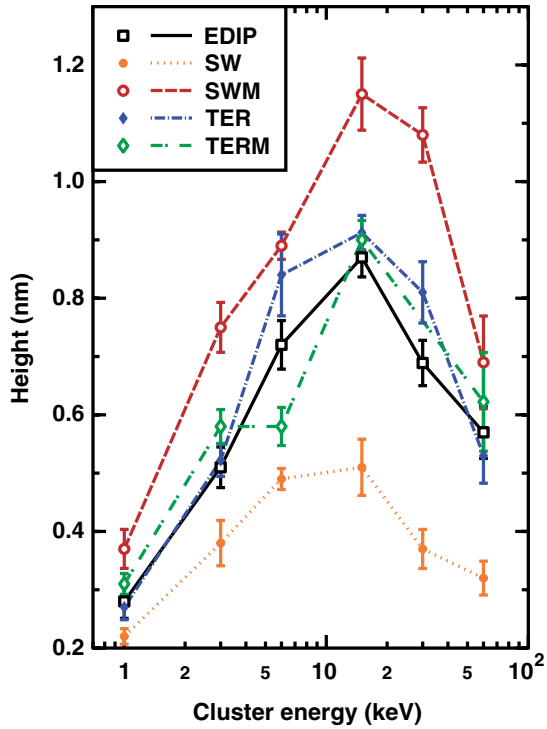


Fig. 3. Average heights of crater rims. Each point represents an average of ten simulations.

single ion bombardment at energies shown in Fig. 1. This also explains that the TERM model shows similar energy

dependence to the other potentials in the single ion simulations.

Fig. 4 shows that there are remarkable differences in shapes of craters produced with different potentials. The potentials produce again very similar energy dependence: Craters are largest between 6 and 30 keV. This indicates that the geometry of the collision cascade is relatively independent of details of the potential. Experimentally observed craters have the same overall energy dependency but they are larger in diameter and can be more complex in size [23]. The reasons for these differences are under investigations.

The diameter of the crater rim depends on energy very much in the same way as Si sputtering yield. This can be seen by comparing Fig. 5 with Fig. 2. Thus, there is correlation between crater area and sputtering yield. TERM is an exception to this behaviour. All potentials give the same qualitative energy dependence for the rim diameter regardless of their functional form.

After cooling of a collision cascade, an amorphous region is left around the crater inside the solid. As we can see in Fig. 6, the depth of this region depends on energy but not on potential. However, the total number of Si atoms in a collision cascade is larger with EDIP and SW than with the other potentials (Fig. 6). The width of the collision cascade is probably related to melting temperature, which is correct with SW and only slightly too low with EDIP. The high melting temperature of Tersoff silicon produces narrower cascades.

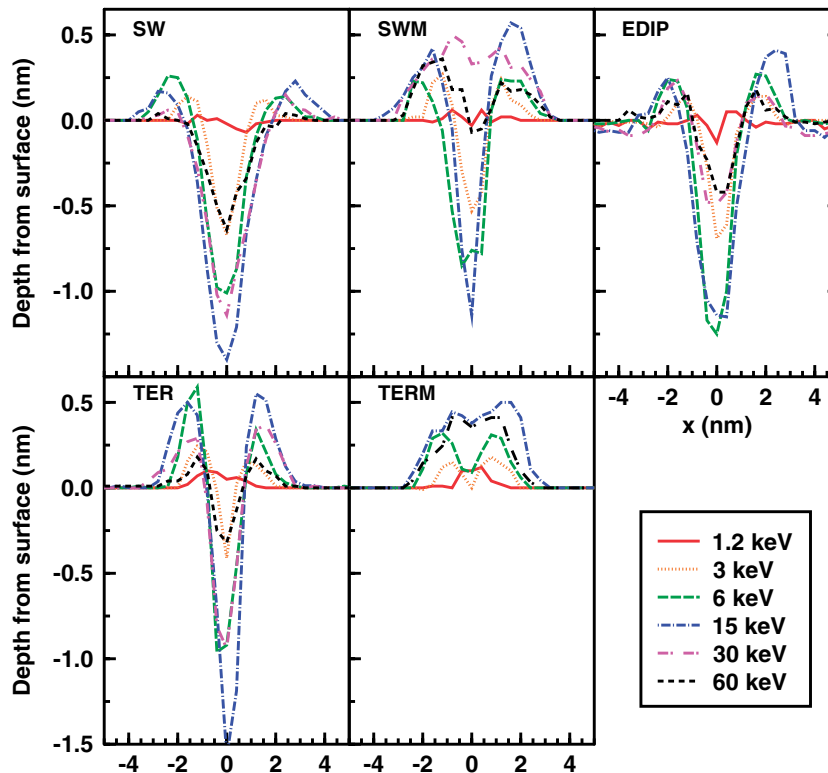


Fig. 4. Profiles of craters at different energies and with different potentials. Each profile is an average of ten simulations. The profiles are calculated when the cascades are cooled, which occurs after 20–40 ps depending on Ar₁₂ cluster energy.

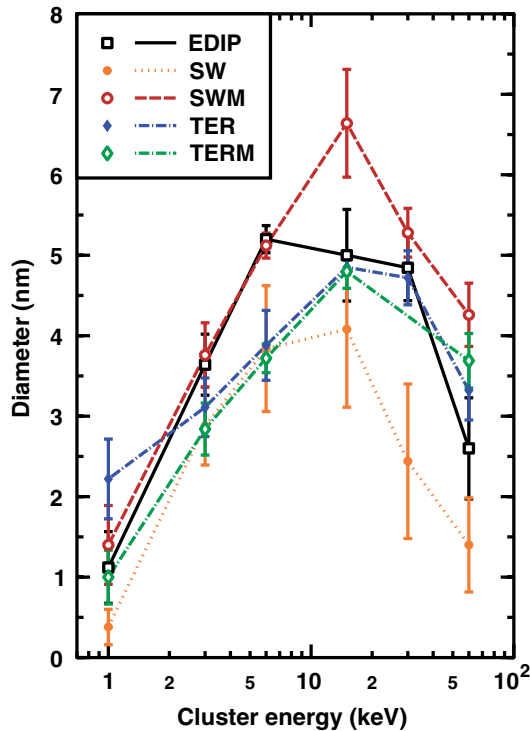


Fig. 5. Average outer diameter of crater rim as a function of Ar_{12} cluster energy. Because rims are not perfectly circular, diameters are measured along two mutually perpendicular directions along.

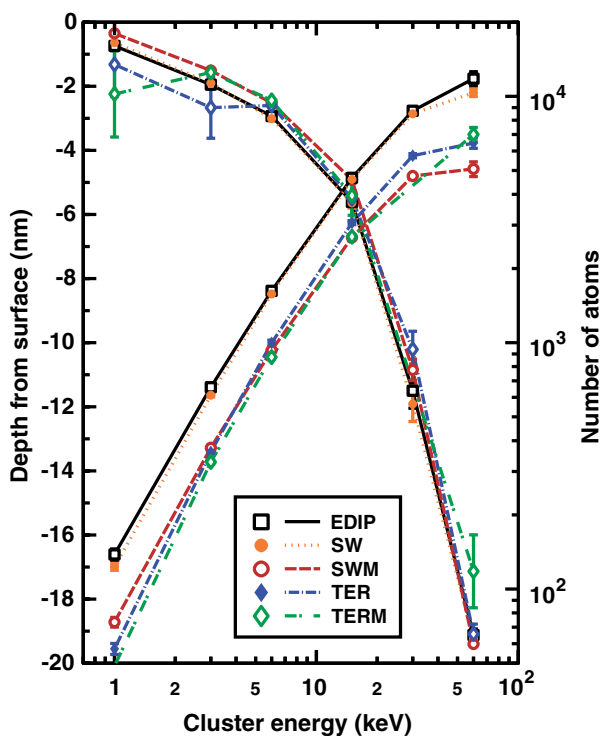


Fig. 6. Average depth of the amorphous regions left after cascades are cooled. Each point represents the average of ten simulations. Also shown the number of atoms displaced in a collision cascade as a function of Ar_{12} cluster energy. Atoms that have moved more than 3 \AA from their original positions are counted.

As the small error bars in Fig. 6 indicate, the depth and volume of a collision cascade does not vary very much between runs. In this respect, a collisions of Ar_{12} cluster can be considered an almost continuum phenomenon, which has little atomic level fluctuations. Furthermore, this predictability, added to the fact that the same cascade depths can be obtained with all potentials, lead us to conclude that collision cascades in Si can be simulated almost equally well with all potentials that describe at least the major characteristics of Si bonding. However, there is no experimental data available to verify whether or not the potentials produce the right size for the amorphous region. This conclusion about potential independence does not hold with sputtering yields and crater dimensions, because these quantities vary with the potential.

5. Conclusions

The potentials tested give almost the same energy dependence for cascades depths and similar energy dependence for crater shapes. We can conclude, that the overall cascade dynamics is not very much dependent on details of the potential provided that the potential describes the main features of Si bonding. However, there is a great variation of details of crater shapes and sputtering yields depending on functional forms and even on the different parametrizations of the same potential.

It is not possible to conclude that one of the potentials is the best for cluster collision simulations. More precise comparisons to experimental data of, for example, crater dimension are required. However, EDIP seems to be a good choice, because it provides single ion sputtering yields which agree quite well with experimental yields at different energies and produces cascades that have about the same size as cascades simulated with SW that gives the correct melting temperature.

Acknowledgements

The research was supported by Finnish Academy of Science and Letters, Vilho, Yrjö and Kalle Väisälä Foundation.

References

- [1] G. Brauchle, S. Richard-Schneider, D. Illig, J. Rockenberger, R.D. Beck, M.M. Kappes, *Appl. Phys. Lett.* 67 (1995) 52.
- [2] L.P. Allen, Z. Insepov, D.B. Fenner, C. Santeufemio, W. Brooks, K.S. Jones, I. Yamada, *J. Appl. Phys.* 92 (2002) 3671.
- [3] V. Popok, S. Prasalovich, E. Campbell, *Surf. Sci.* 556 (2004) 1179.
- [4] A.S. Dalton, E.G. Seebauer, *Surf. Sci.* 550 (2003) 140.
- [5] R. Vink, G. Barkemay, W. van der Wegz, N. Mousseaux, *J. Non-Cryst. Solids* 282 (2001) 248.
- [6] F.H. Stillinger, T.A. Weber, *Phys. Rev. B* 31 (1985) 5262.
- [7] F.H. Stillinger, T.A. Weber, *Phys. Rev. B* 33 (1986) 1451.
- [8] W.D. Luedtke, U. Landman, *Phys. Rev. B* 37 (1988) 4656.
- [9] W.D. Luedtke, U. Landman, *Phys. Rev. B* 40 (1989) 1164.
- [10] H. Balamane, T. Halicioglu, W.A. Tiller, *Phys. Rev. B* 46 (1992) 2250.

- [11] J.Q. Broughton, X.P. Li, Phys. Rev. B 35 (1987) 9120.
- [12] U. Landman, W.D. Luedtke, R.N. Barnett, C.L. Cleveland, E. Arnold, S. Ramesh, H. Baumgart, A. Martinez, B. Khan, Phys. Rev. Lett. 56 (1986) 155.
- [13] J. Tersoff, Phys. Rev. B 37 (1988) 6991.
- [14] J. Tersoff, Phys. Rev. B 38 (1988) 9902.
- [15] S.J. Cook, P. Clancy, Phys. Rev. B 47 (1993) 7686.
- [16] M. Ishimaru, K. Yoshida, T. Motooka, Phys. Rev. B 53 (1996) 7176.
- [17] B.J. Thijsse, T.P.C. Klaver, E.F. Haddeman, Appl. Surf. Sci. 231 (2004) 29.
- [18] J.F. Justo, M.Z. Bazant, E. Kaxiras, V.V. Bulatov, S. Yip, Phys. Rev. B 58 (1998) 2539.
- [19] J. Samela, J. Kotakoski, K. Nordlund, J. Keinonen, Nucl. Instr. and Meth. B 239 (2005) 331.
- [20] J.F. Ziegler, J.P. Biersack, U. Littmark, The Stopping and Range of Ions in Matter, Pergamon, New York, 1985.
- [21] K. Nordlund, Comput. Mater. Sci. 3 (1995) 448.
- [22] K. Wittmaack, Phys. Rev. B 68 (2003) 235211.
- [23] S. Prasalovich, V. Popok, P. Persson, E.E. Campbell, Eur. Phys. J. D 36 (2005) 79.